A Stochastic Linearization Approach to Optimal Primary Control of Power Systems with Generator Saturation

Sarnaduti Brahma, Mads R. Almassalkhi and Hamid R. Ossareh

***Abstract*— Quasilinear Control (QLC) is a set of methods used for analysis and design of systems with nonlinear actuators and sensors. It is based on the method of stochastic linearization, which replaces a nonlinearity by an equivalent gain and bias. Here, we leverage QLC to systematically design an optimal droop controller for primary frequency control of power systems with asymmetric generator saturation and renewable penetration. The droop parameters are found by solving an optimization problem wherein the cost function is a combination of the change in frequency and the actuator input. Simulation studies show that the combined output and control cost is improved compared to a baseline design, and that the systematic design process provides an appropriate response to any change in input or system parameters.**

I. Introduction

Control of frequency in power systems is vital to ensure reliable operation. In a power system, the frequency can deviate from the nominal value when there is a mismatch between supply and demand, which could result from changes in demand, tripping of generators, or isolation of areas with large generation capacity. A poorly controlled power system would result in a low quality of supplied electrical energy that can lead to power system collapse. Hence, power systems are typically equipped with an automatic frequency control system that nullifies any change in frequency.

An automatic frequency control system is generally implemented in three parts: primary, secondary and tertiary control [1]–[3]. Primary Frequency Control (PFC), or droop control, which is the focus of this paper, serves to bring the frequency back to an acceptable value locally in a power system area, although leaving a steady state error in frequency due to the purely proportional droop controller. This control task is shared by all generators in the area, irrespective of the location of the disturbance.

The proportional droop controller used in primary control can be chosen optimally. This can ensure, for example, a minimal change in frequency with reduced control effort. Optimized droop control has been studied in the literature. For example, Mallada et. al [5] propose an optimal load-side frequency control mechanism to maintain the grid within operational constraints. In [6] and [7] averaging-based distributed controllers, using communication among the generation units to ensure economic optimization, are explored. A distributed real time frequency control scheme, using reverse and forward engineering, is discussed in [8]. In [9], dynamic droop controllers that improve the dynamics without affecting the steady state solution are proposed. In [10], the tracking of an operating point subject to power balance over the network is optimized. Delays in frequency dependent flexible loads are investigated in [11].

The authors are with the Department of Electrical and Biomedical Engineering, The University of Vermont, Burlington, VT 05405, U.S.A. Email: {sbrahma, malmassa, hossareh}@uvm.edu

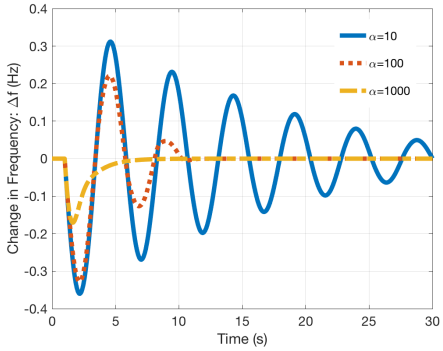

Fig. 1. Effect of actuator saturation on droop control - A highly saturated actuator (α=10) leads to oscillations in the frequency deviations from the nominal for a step change in load power. A less saturated actuator ($\alpha = 100$) leads to less oscillations. With negligible saturation ($\alpha = 1000$), the response is overdamped. Note that a small steady state error is present in this case, although not visible to the naked eye. This is for illustration only, with system parameters taken from [4].

These references, however, do not *systematically* incorporate the issue of generator power saturation, which can take place when, for example, the gate or valve position that influences the flow of steam into a turbine is restricted, leading to specific output power limits. By *systematically*, we mean a design process that explicitly considers all the system parameters including saturation limits and, at the same time, does not lead to overly complex controllers. While neglecting saturation leads to simplification in the controller design and analysis, the results obtained may not accurately reflect the performance when saturation is present.

We illustrate this fact using a simulation analysis, where the same droop controller is used with varying levels of saturation (we used the system given in [4]). As shown in Fig. 1 by the orange dashed line, an unsaturated actuator leads to a well-behaved droop response - a momentary change in frequency, caused due to a step change in load power, is brought back to a constant value without oscillations. However, when there is significant generator saturation, the frequency change shows an underdamped response before being nullified, as shown by the solid line.

The above example motivates the systematic design of an optimal droop controller to account for generator saturation in power systems. In general, actuator saturation is a nonlinearity that cannot be linearized in the traditional

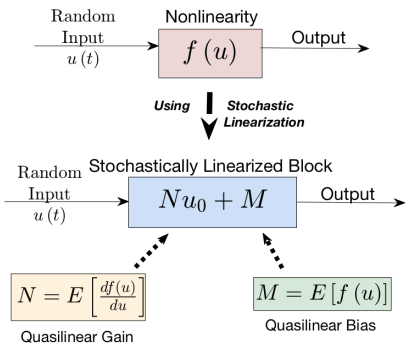

Fig. 2. Stochastic Linearization - the method used in Quasilinear Control. Here, $E[\cdot]$ is the expectation operator, and u_0 is the zero-mean part of u, i.e., $u_0 = u - E[u]$.

sense because large inputs saturate the actuator. While plants are also nonlinear, they can usually be linearized around an operating point if the control system is well-designed.

Quasilinear control (QLC) is a set of methods that can be applied to analyze and optimize such nonlinear systems [12]–[14]. It employs a mathematical technique referred to as stochastic linearization [15]–[18], which uses statistical properties of stochastic inputs to linearize the system, as shown in Fig. 2. This contrasts with classical describing function analysis [19], which replaces the nonlinearity by a describing function whose gain is a function of the (deterministic) sinusoidal input amplitude. In [20], for example, the method of QLC has been applied to control a wind farm power output. Each turbine has been modeled by a linear plant preceded by an asymmetric saturation nonlinearity accounting for the limited availability of wind, which acts as a random input.

In this paper, we leverage the method of QLC to systematically design an optimal droop controller that will dynamically adapt to the system parameters. Numerical simulations show that the resulting optimal QLC controller reduces the combined state and control costs by as much as 17% compared to a baseline design from the literature. Since QLC depends on all the parameters of the system, any change in a parameter leads to a systematic redesign of the optimal controller to meet performance requirements.

The organization of the paper is as follows. In Section II, the system model is described and the optimization problem formulated. The description of the QLC design procedure is given in Section III. Section IV illustrates the design process using numerical simulations. Section V concludes the paper with a summary and topics for future research.

II. Modeling and Problem Formulation

A. Primary Frequency Control in Power Systems

Consider a simple two-area power system, which appears in [4] and is shown in Fig. 3. This is a simplified model to represent the dominant behavior of a large, interconnected power system having many control zones. It consists of two single-bus systems Σ_1 and Σ_2, each characterized by six parameters and connected with a tie-line in between

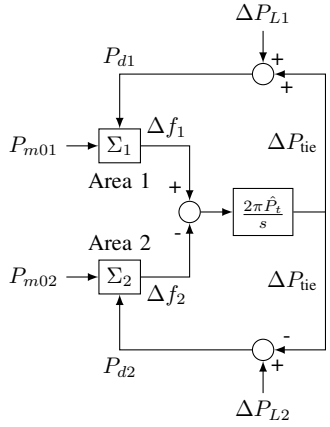

Fig. 3. Block diagram of primary frequency control of a two-area interconnected power system

them. The block diagram of system Σ_i is shown in Fig. 4a. Here the parameter T_{ti} represents the effective time constant of the governor/turbine dynamics, and H_i the total inertia constant of the area, which is rated at the base power S_{bi}. The parameter D_{Li} models the motor loads and W_{0i} the frequency-dependent loads. Finally, the parameter S_i, also known as speed regulation or droop, determines the effective steady-state speed vs. load characteristic of the generating units. Modifying this parameter affects the proportional droop controller gain $1/S_i$, thereby regulating the change in frequency from the nominal value of f_0. The block $\text{sat}_{\alpha_i}^{\beta_i}(u_i)$ models the saturating actuator and is explained in II-B. Each individual control area Σ_i has effectively two inputs, the mechanical power set-point P_{m0i} and the effective change in load power P_{di}, which acts as a power disturbance. The change in frequency Δf_i is the controlled output. As shown in Fig. 3, any mismatch in frequency between the two areas gives rise (through the block modeled by the parameter $\hat{P}_t$ related to the tie-line reactance) to a power flow ΔP_{tie} between the two areas. This power, when combined with the local load power disturbance ΔP_{Li} and fed back as the effective change in load power P_{di} to each area, regulates the frequency to a new steady state value, according to the following equations:

$$P_{d1} = \Delta P_{L1} + \Delta P_{\text{tie}} \quad \text{and} \quad P_{d2} = \Delta P_{L2} - \Delta P_{\text{tie}}$$

B. Nonlinearity in the Actuator

In the block diagram of Fig. 4a, it is assumed that the turbine output u_i, which is the change in mechanical power, is saturated by an asymmetric saturation nonlinearity, shown in Fig. 5. This situation can arise, for example, when the position of the gate or valve controlling the flow of steam into the turbine is restricted, resulting in specific power limits. The saturation is assumed to be asymmetric, with an upper bound $\beta_i > 0$ and a lower bound $\alpha_i < 0$, such that $|\alpha_i| > |\beta_i|$. This is a reasonable assumption since a turbine nominally produces mechanical power P_0 close to its designed capacity, $P_0 + \beta_i$. In the event of a frequency deviation, it can thus produce an output power between $P_0+\alpha_i < P_0$ and $P_0+\beta_i > P_0$. Since this model is linearized

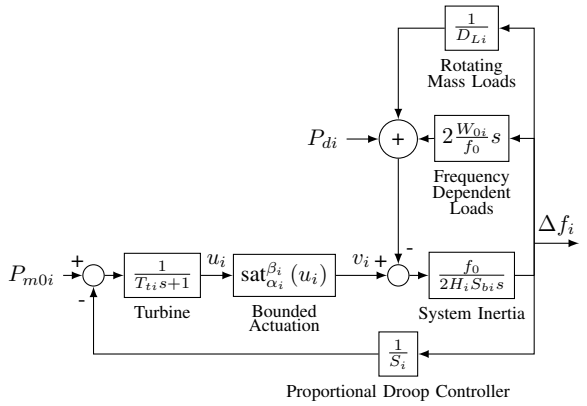

(a) Block diagram of each control area Σ_i

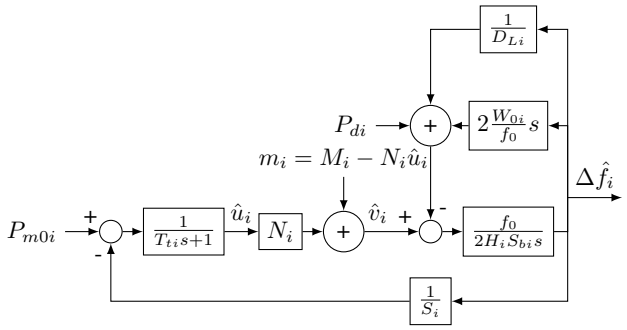

(b) Stochastically linearized system corresponding to Fig. 4a

Fig. 4. Droop Control System

around the nominal power P_0, the change in mechanical power output v_i of turbine is restricted between α_i and β_i, as modeled by the asymmetric saturation. Note that in this paper, v_i does not refer to voltage, but we are using this notation to be consistent with earlier works in the literature of QLC.

C. Problem Statement

The problem is to design optimal droop parameters S_1, S_2 that would improve the combined frequency and actuator input performance of the power system, compared to a baseline design, should any frequency deviation take place. This involves using stochastic linearization to find an equivalent quasilinear system, selecting a suitable cost function to minimize and then optimizing over an admissible region to find the optimal droop parameters. These are done in the sections to follow.

III. QLC Based Droop Controller Design

In this section, the method of QLC is leveraged to design the optimal droop controller. It is appropriate to do so in this context since the load disturbance in power systems is stochastic in nature and QLC requires that all exogenous inputs to the system be random processes. The change in load power is thus first modeled accordingly. The nonlinear actuator block is then replaced by the corresponding stochastically linearized block for further analysis. The design process is explained below.

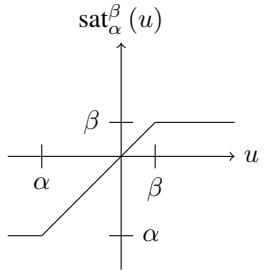

Fig. 5. Asymmetric Saturation Nonlinearity

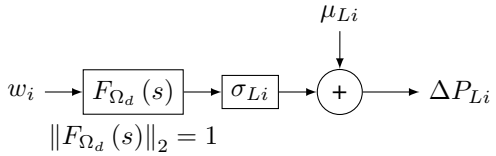

Fig. 6. Modeling the change in load power

A. Modeling the Load Power Disturbance

The change in load power ΔP_{L_i} in area i is modeled as a wide sense stationary Gaussian white noise with mean μ_{Li} and standard deviation σ_{Li}. The Gaussian distribution is a reasonable modeling assumption for a power system load disturbance having small temporal scales due to the central limit theorem and has been used in [20] to model wind farm power disturbance. Similar reasoning can be applied in solar applications. The noise ΔP_{L_i} is modeled as a standard white Gaussian noise w_i, as shown in Fig. 6, passed through a coloring filter $F_{\Omega_d}(s)$ of bandwidth Ω_d, multiplied by a gain σ_{Li}, and added to a bias μ_{Li}. To ensure a realistic disturbance signal, the filter bandwidth is chosen to equal the closed loop bandwidth of the control area for the system to be able to detect the change in load power. Also, by choosing the filter such that its H_2-norm equals unity, the final signal ΔP_{Li} is ensured to have mean μ_{Li} and standard deviation σ_{Li}.

B. Stochastic Linearization of the Nonlinear Actuator

To analyze the system and determine the optimal droop parameters, the nonlinear actuator needs to be linearized. The method of stochastic linearization leveraged here utilizes the statistical properties of the disturbance signal to linearize the system. As shown in [12], this is superior to the usual method of Jacobian linearization for this class of nonlinear systems. This is because the stochastically linearized block depends on all elements of the closed loop system. The method of QLC thus provides a more faithful picture of the entire system, contrary to Jacobian linearization, where the linear block depends only on the nonlinear element and the operating point.

Stochastic linearization considers a nonlinear system described by the following input-output relationship:

$$v(t) = f(u(t))$$

where $u(t)$ is the input random process, $v(t)$ is the output and $f(\cdot)$ is a piecewise differentiable function. Stochastic linearization [13], [21] reduces this system to an equivalent

linear system described by (see also Fig. 2):

$$\hat{v}(t) = Nu_0(t) + M$$

where $u_0(t) = u(t) - \mu_u$ is the zero-mean part of the input $u(t)$, μ_u the mean of $u(t)$ and $\hat{v}(t)$ the new output. Here the parameter N is called the quasilinear gain and M the quasilinear bias. They are calculated using the following equations, which minimize the mean square difference $E[(v-\hat{v})^2]$:

$$N = E\left[\left.\frac{df(u)}{du}\right|_{u=u(t)}\right] \tag{1}$$

$$M = E[f(u(t))] \tag{2}$$

Leveraging the method of stochastic linearization, the nonlinear system of area i described by Fig. 4a can be reduced using equations (1) and (2) to an equivalent linear system shown in Fig. 4b, where the nonlinearity $\text{sat}_{\alpha_i}^{\beta_i}$ has been replaced by an equivalent quasilinear gain N_i and a bias $m_i = M_i - N_i\mu_{\hat{u}_i}$ such that M_i is the quasilinear bias and $\mu_{\hat{u}_i}$ the mean of actuator input. Here,

$$N_i = \frac{1}{2}\left[\text{erf}\left(\frac{\beta_i - \mu_{\hat{u}_i}}{\sqrt{2}\sigma_{\hat{u}_i}}\right) - \text{erf}\left(\frac{\alpha_i - \mu_{\hat{u}_i}}{\sqrt{2}\sigma_{\hat{u}_i}}\right)\right] \tag{3}$$

and

$$M_i = \frac{\alpha_i + \beta_i}{2} + \frac{\mu_{\hat{u}_i} - \beta_i}{2}\text{erf}\left(\frac{\beta_i - \mu_{\hat{u}_i}}{\sqrt{2}\sigma_{\hat{u}_i}}\right)$$

$$-\frac{\mu_{\hat{u}_i} - \alpha_i}{2}\text{erf}\left(\frac{\alpha_i - \mu_{\hat{u}_i}}{\sqrt{2}\sigma_{\hat{u}_i}}\right) - \frac{\sigma_{\hat{u}_i}}{\sqrt{2\pi}}\left\{\exp\left[-\left(\frac{\beta_i - \mu_{\hat{u}_i}}{\sqrt{2}\sigma_{\hat{u}_i}}\right)^2\right]\right.$$

$$\left. - \exp\left[-\left(\frac{\alpha_i - \mu_{\hat{u}_i}}{\sqrt{2}\sigma_{\hat{u}_i}}\right)^2\right]\right\} \tag{4}$$

where $\sigma_{\hat{u}_i}$ is the standard deviation of $\hat{u}_i$, $\hat{u}_i$ is the actuator input in the stochastically linearized system, and

$$\text{erf}(x) = \frac{2}{\sqrt{\pi}}\int_0^x e^{-t^2}dt$$

is the error function. Recall that α_i and β_i are the generator saturation limits in area i. For more details, please refer to [12], [20].

As seen from equations (3) and (4), calculation of N_1, N_2, M_1 and M_2 requires knowledge of $\mu_{\hat{u}_1}$, $\mu_{\hat{u}_2}$, $\sigma_{\hat{u}_1}$ and $\sigma_{\hat{u}_2}$. Since the system is interconnected, these values depend on each other. For the sake of illustration, we assume that the disturbance in load power takes place only in the first area, i.e., $\Delta P_{L2} = 0$. Considering that the system is operating in the stationary regime, the values of $\sigma_{\hat{u}_1}$ and $\sigma_{\hat{u}_2}$ can be found using the transfer function $T_1(s)$ from the change in load power ΔP_{L1} to the actuator input $\hat{u}_1$:

$$\sigma_{\hat{u}_1} = \|F_{\Omega_d}(s)\,T_1(s)\|_2\,\sigma_{L1} = f_1(N_1, N_2, S_1, S_2) \tag{5}$$

where $\|\cdot\|_2$ is the H_2-norm. Similarly, using the transfer function $T_2(s)$ from the change in load power ΔP_{L1} to the second actuator input $\hat{u}_2$:

$$\sigma_{\hat{u}_2} = \|F_{\Omega_d}(s)\,T_2(s)\|_2\,\sigma_{L1} = f_2(N_1, N_2, S_1, S_2) \tag{6}$$

The values of $\mu_{\hat{u}_1}$ and $\mu_{\hat{u}_2}$ can be found by first finding the transfer functions from P_{m01}, P_{m02}, μ_{L1}, m_1 and m_2 to $\hat{u}_1$ and $\hat{u}_2$ and then evaluating the DC gains, which leads to:

$$\mu_{\hat{u}_1} = P_{m01} + \frac{L}{S_1} = f_3(M_1, M_2, S_1) \tag{7}$$

$$\mu_{\hat{u}_2} = P_{m02} + \frac{L}{S_2} = f_4(M_1, M_2, S_2) \tag{8}$$

where:

$$L = \frac{D_{L1}D_{L2}}{D_{L1} + D_{L2}}(\mu_{L1} - M_1 - M_2) \tag{9}$$

The values of N_1, N_2, M_1 and M_2 can thus be found by substituting (5)-(9) into (3) and (4), which results in a system of four transcendental equations in the four unknowns N_1, N_2, M_1 and M_2. MATLAB's `fsolve` command provides a convenient way to solve this numerically.

C. Selection of Suitable Cost Function

To find an optimal controller, a suitable cost function is required. It is desirable to have small change in frequency and low actuator input. Several possible objective functions were plotted as a function of the droop parameters S_1 and S_2, which are the optimization variables. In each case, actuator saturation was neglected, as it mainly serves to impose constraints and does not change the nature or shape of the cost function. Also, no change in load power of area 2 was assumed, i.e., $\Delta P_{L2} = 0$.

An objective function defined as the sum of variances of frequency deviations in the two areas, i.e., $\sigma^2_{\Delta\hat{f}_1} + \sigma^2_{\Delta\hat{f}_2}$, results in a surface shown in Fig. 7. Note that $\Delta\hat{f}_i$ are the outputs of the stochastically linearized system shown in Fig. 4b. For plotting this surface, the values of $\sigma_{\Delta\hat{f}_1}$ and $\sigma_{\Delta\hat{f}_2}$ were calculated using the following equations, similar to equations (5) and (6):

$$\sigma_{\Delta\hat{f}_1} = \|F_{\Omega_d}(s)\,T_3(s)\|_2\,\sigma_{L1}$$

$$\sigma_{\Delta\hat{f}_2} = \|F_{\Omega_d}(s)\,T_4(s)\|_2\,\sigma_{L1}$$

where $T_3(s)$ and $T_4(s)$ are the transfer functions from ΔP_{L1} to $\Delta\hat{f}_1$ and $\Delta\hat{f}_2$ respectively.

The surface has an infimum at zero, leading to infinite gain in the proportional controller, as the control action is not penalized. A surface similar to that of Fig. 7 results when the objective function is defined as the sum of variances of frequency deviations: $\Delta\hat{f}_1$ and $\Delta\hat{f}_1$, and also the variances of rate of change of frequency (ROCOF): $\frac{d}{dt}\left(\Delta\hat{f}_1\right)$ and $\frac{d}{dt}\left(\Delta\hat{f}_2\right)$. Unlike the surface in Fig. 7, the surface shown in Fig. 8, which is generated using the objective function defined as the sum of variances of changes in frequency and lowly penalized variances of actuator inputs, is more suitable for implementation. This is because the surface has a specific minimum leading to a finite controller gain unlike the other. Hence, this surface is chosen for formulating the optimization problem, as explained in the following subsection. This is also consistent with standard practice in optimal control, for example in designing a linear quadratic

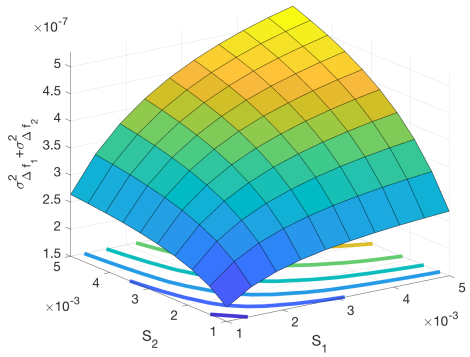

Fig. 7. Surface contour plot of objective function $\sigma^2_{\Delta f_1}+\sigma^2_{\Delta f_2}$ neglecting actuator saturation. The surface can be seen to have an infimum at the origin.

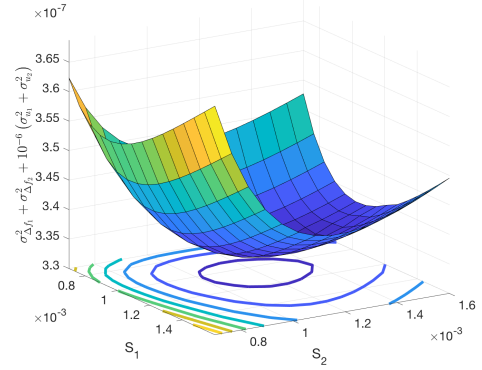

Fig. 8. Surface contour plot of objective function $\sigma^2_{\Delta f_1}+\sigma^2_{\Delta f_2}+10^{-6}\left(\sigma^2_{u_1}+\sigma^2_{u_2}\right)$ neglecting actuator saturation. The non-zero minimum of this surface allows for the design of a finite controller gain compared to the surface of Fig. 7.

regulator (LQR), which optimizes the combined state and control costs for a system.

D. Optimization Problem

Using the surface explained in the previous subsection, the optimization problem is formulated as:

$$\begin{aligned}&\min_{S_1,S_2}\ \sigma^2_{\Delta\hat{f}_1}+\sigma^2_{\Delta\hat{f}_2}+\rho\left(\sigma^2_{\hat{u}_1}+\sigma^2_{\hat{u}_2}\right)\\&\text{subject to (3)–(8) and } S_1,S_2>0\end{aligned}\tag{10}$$

where $\rho>0$ is a sufficiently small scalar. Since this problem is non-convex, with transcendental constraints (3) and (4), it cannot be solved analytically. However, it can be approached numerically, for example, using MATLAB's `lsqnonlin` command.

IV. Performance Evaluation and Discussion of Results

To evaluate the performance of the designed optimal controller, the two-area power system in Fig. 3 was simulated for a sufficiently long time, first with droop parameters from the baseline design of [4], and then with the designed optimal QLC controller. The value of ρ for the optimization was 1.27×10^{-8}, which was selected by analyzing the Pareto optimal front discussed below. The system parameters of area 2 were chosen to equal those of area 1, as in Table I, so that both areas were of the same size. In both cases, the load power change in area 1 was modeled as a zero-mean white Gaussian noise with a standard deviation of σ_{L1} =200 MW, passed through a 3rd-order Butterworth filter $F_{\Omega_d}(s)$, with bandwidth Ω_d chosen to be the same as the closed loop bandwidth of one of the power system areas (around 0.56 Hz):

TABLE I

Parameters and their values used for Simulation

Parameter	Value
$H_1=H_2$	5 s
$S_{b1}=S_{b2}$	10 GW
f_0	50 Hz
$D_{l1}=D_{l2}$	$\frac{1}{200}$ Hz/MW
$W_{01}=W_{02}$	0 MW/Hz
$S_1=S_2$	$\frac{1}{5000}$ Hz/MW
$\hat{P}_t$	533.33 MW

$$F_{\Omega_d}(s)=\sqrt{\frac{3}{\Omega_d}}\left(\frac{\Omega_d^3}{s^3+2\Omega_d s^2+2\Omega_d^2 s+\Omega_d^3}\right),\Omega_d=0.56\text{ Hz}\tag{11}$$

For illustration, the load power change in the second area was assumed to be zero. For both areas, the value of α was chosen to be -100 MW and $\beta=5$ MW, so that the saturation is asymmetric as explained in Section II-B.

The numerical optimization required trying several initial conditions before converging to the global minimum. The results, tabulated in Table II, show that the optimal droop parameters reduced the objective function from 0.0197 to 0.0164, i.e., by 17%, compared to the baseline design. Note that the optimization results in an increase in S_2 (i.e., a decrease in $\frac{1}{S_2}$), which is reasonable, since the disturbance does not dynamically affect the second area as much as it does the first area. Although the sum of variances of changes in frequency (i.e., the state cost) increased by 4% from 0.0152 to 0.0158, the control effort reduced by 88% from 34.74×10^4 to 4.05×10^4. Hence, this optimal controller achieves a minimal combined state and control cost at the expense of a slight increase in state cost.

To demonstrate the trade-off between state and control costs, a Pareto optimal front was generated by varying the control penalty from $\rho=10^{-10}$ to $\rho=10^{-5}$, computing the quasilinear gains and biases for each ρ, and calculating the resulting costs using the QLC equations. The result is depicted by the curve in Fig. 9, where the optimal QLC gains are shown to produce a reduced combined cost compared to those in the baseline design of [4]. Note from Fig. 9 that, in contrast to the data above, the QLC equations predict a *reduction* in the state cost compared to the baseline design. This discrepancy is due to the inaccuracy of stochastic linearization for highly asymmetric systems [13], which will be a topic of future investigation. Nevertheless, at the optimum, the state cost of the nonlinear system is 0.0247, while that of the stochastically linearized version is 0.0231, indicating the high accuracy of stochastic linearization.

To illustrate the fact that QLC allows us to *systematically* redesign the controller upon parameter changes, we performed the following experiment. We assumed that σ_{L1} in

TABLE II

SYSTEM PARAMETERS BEFORE AND AFTER OPTIMIZATION

Parameter	Baseline	Optimal
S_1	0.00020	0.0006
S_2	0.00020	50.6705
N_1	0.0694	0.1979
N_2	1.0000	1.0000
M_1	-44.1950	-37.9331
M_2	0.0011	0.0000
$\sigma^2_{\Delta f_1} + \sigma^2_{\Delta f_2}$	0.0152	0.0158
$\sigma^2_{\Delta \hat{f}_1} + \sigma^2_{\Delta \hat{f}_2}$	0.0156	0.0160
$\sigma^2_{\Delta f_1} + \sigma^2_{\Delta f_2} + \rho\left(\sigma^2_{u_1} + \sigma^2_{u_2}\right)$	0.0197	0.0164
$\sigma^2_{\Delta \hat{f}_1} + \sigma^2_{\Delta \hat{f}_2} + \rho\left(\sigma^2_{\hat{u}_1} + \sigma^2_{\hat{u}_2}\right)$	0.0201	0.0166

the previous experiment increased from 200 MW to 300 MW due to, for example, increased renewable penetration. If the same QLC-based droop parameters are applied, the optimal value of the cost function increases from 0.0164 to 0.0481. This increase is reasonable, because a larger input forces the system to operate closer to its limits, which constrains achievable performance. However, if the droop parameters are re-designed with the new information on σ_{L1}, the value of the cost function is lowered to 0.0479, a decrease by 0.5%. Note that this decrease is small compared to that in the previous case, since the optimization is being performed on an already optimal QLC-based controller produced using $\sigma_{L1} = 200$ MW. This experiment illustrates the effectiveness of QLC in systematically redesigning controllers based on available information on system parameters, which can be found out experimentally.

V. CONCLUSION

In this paper, the method of QLC has been applied to design an optimal droop controller for primary frequency control of power systems with generator saturation. Numerical simulations show that the controller achieves a reduced combined state and control cost, compared to a baseline design, at the expense of a slightly increased state cost. Since the process depends on the values of all the system parameters, the optimal controller can dynamically update itself on change of parameters, for example, the load variability or the saturation limits, to produce optimal performance. Future work includes the application of QLC to saturation in slew rate, the numerical stability and robustness of the QLC design, application to power systems with more areas and distributed renewable generation, and accuracy of stochastic linearization.

ACKNOWLEDGMENT

The authors acknowledge funding by the United States Department of Energy, Award DE-EE000008006.

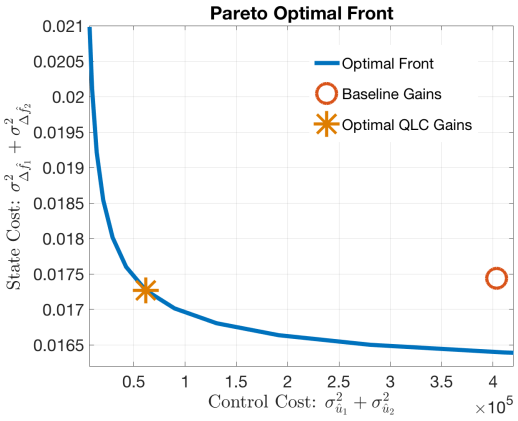

Fig. 9. Pareto optimal front of cost function with ρ ranging logarithmically from 10^{-10} to 10^{-5}.

REFERENCES

[1] P. Kundur, *Power Systems Stability and Control*, 1994.

[2] A. J. Wood and B. F. Wollenberg, *Power Generation, Operation, and Control*, 1996, vol. 37, no. 2.

[3] P. Sauer, M. Pai, and J. Chow, *Power System Dynamics and Stability: With Synchrophasor Measurement and Power System Toolbox*, 2017.

[4] G. Anderson, "Dynamics and Control of Electric Power Systems," *Lecture 227-0528-00, ITET ETH*, no. February, pp. 32–35, 2012.

[5] E. Mallada, C. Zhao, and S. Low, "Optimal Load-Side Control for Frequency Regulation in Smart Grids," *IEEE Transactions on Automatic Control*, vol. 62, no. 12, pp. 6294–6309, dec 2017. [Online]. Available: http://ieeexplore.ieee.org/document/7944568/

[6] F. Dörfler, J. Simpson-Porco, and F. Bullo, "Breaking the Hierarchy: Distributed Control & Economic Optimality in Microgrids," jan 2014.

[7] F. Dorfler, J. W. Simpson-Porco, and F. Bullo, "Plug-and-play control and optimization in microgrids," in *Proceedings of the IEEE Conference on Decision and Control*, vol. 2015-Febru, no. February. IEEE, dec 2014, pp. 211–216. [Online]. Available: http://ieeexplore.ieee.org/document/7039383/

[8] S. You and L. Chen, "Reverse and forward engineering of frequency control in power networks," in *53rd IEEE Conference on Decision and Control*. IEEE, dec 2014, pp. 191–198. [Online]. Available: http://ieeexplore.ieee.org/document/7039380/

[9] E. Mallada, "IDroop: A Dynamic Droop controller to decouple power grid's steady-state and dynamic performance," in *2016 IEEE 55th Conference on Decision and Control, CDC 2016*. IEEE, dec 2016, pp. 4957–4964. [Online]. Available: http://ieeexplore.ieee.org/document/7799027/

[10] C. Zhao, U. Topcu, N. Li, and S. Low, "Design and stability of load-side primary frequency control in power systems," *IEEE Transactions on Automatic Control*, vol. 59, no. 5, pp. 1177–1189, may 2014. [Online]. Available: http://arxiv.org/abs/1305.0585 http://dx.doi.org/10.1109/TAC.2014.2298140

[11] M. Amini and M. Almassalkhi, "Investigating delays in frequency-dependent load control," in *IEEE PES Innovative Smart Grid Technologies Conference Europe*. IEEE, nov 2016, pp. 448–453. [Online]. Available: http://ieeexplore.ieee.org/document/7796427/

[12] S. Ching, Y. Eun, C. Gokcek, P. T. Kabamba, and S. M. Meerkov, *Quasilinear Control*. Cambridge: Cambridge University Press, 2010. [Online]. Available: http://ebooks.cambridge.org/ref/id/CBO9780511976476

[13] P. Kabamba, S. Meerkov, and H. Ossareh, "Stochastic linearisation approach to performance analysis of feedback systems with asymmetric nonlinear actuators and sensors," *International Journal of Control*, vol. 88, no. 1, pp. 65–79, 2015. [Online]. Available: http://www.tandfonline.com/doi/abs/10.1080/00207179.2014.938300

[14] H. R. Ossareh, "An LQR theory for systems with asymmetric saturating actuators," in *Proceedings of the American Control Conference*, ser. 2016 American Control Conference (ACC), vol. 2016-July. IEEE, jul 2016, pp. 6941–6946. [Online]. Available: http://ieeexplore.ieee.org/document/7526766/

[15] R. C. Boonton, "Nonlinear control systems with random inputs," *IRE Trans. on Circuit Theory*, vol. 1, pp. 9–18, 1954.

[16] A. Gelb and W. E. Vander Velde, *Multiple input describing function and nonlinear design*. New York: McGraw-Hill, 1968.

[17] I. E. Kazakov, "An approximate method for the statistical investigation of nonlinear systems," *Trudi Voenno-Vazdusknoi Inzhenernoi Akademii Imeni Prof. N. E. Zhukovskogo*, vol. 399, pp. 1–52, 1954.

[18] I. E. Kazakov and B. G. Dostupov, *Statistical Dynamics of Nonlinear Control Systems*. Fizmatgiz, 1962.

[19] H. K. Khalil, *Nonlinear Systems*, 3rd ed. Prentice Hall, 2002.

[20] Y. Guo, P. T. Kabamba, S. M. Meerkov, H. R. Ossareh, and C. Y. Tang, "Quasilinear Control of Wind Farm Power Output," *IEEE Transactions on Control Systems Technology*, vol. 23, no. 4, pp. 1555–1562, 2015.

[21] J. B. Roberts and P. D. Spanos, *Random Vibrations and Statistical Linearization*, 1990.